Contemporaneous intraplate magmatism on conjugate South Atlantic margins: a hotspot conundrum

André R. Guimarães[a], J. Godfrey Fitton[a*], Linda A. Kirstein[a], Dan N. Barfod[b]

[a]School of GeoSciences, University of Edinburgh, James Hutton Road, Edinburgh EH9 3FE, UK

[b]NERC Argon Isotope Facility, Scottish Universities Environmental Research Centre, Rankine Avenue, East Kilbride, G75 0QF, UK

*Correspondence to: godfrey.fitton@ed.ac.uk

Abstract

Intraplate magmatism is enigmatic in origin despite its importance in our understanding of crustal cycling through the deep mantle. A mantle plume origin is justified for some intraplate magmatism, but not in the case of a large number of occurrences. Here we present a novel explanation for intraplate magmatism in situations where evidence for a plume origin is either lacking or equivocal. Specifically, we highlight two voluminous, long-lived intraplate magmatic provinces located on the precisely conjugate continental margins of Cameroon and NE Brazil and which lasted, respectively, from 65 and 52 Ma to the present. New Ar dating and geochemical data show that magmatism in the two provinces was contemporaneous, identical in incompatible-element composition, and started >40 Myr after continental separation, when the two margins were ~2000 km apart. Lack of age progression in magmatic activity rules out a mantle plume origin. We propose an origin in sub-continental lithospheric mantle that was thickened during Gondwana supercontinent assembly. Thermal re-equilibration of the thickened lithosphere accompanied by percolation of carbonate-rich melt led to the formation of a thick zone of newly created, enriched asthenosphere that is held in place by buoyancy, prevented from dispersing by adjacent lithospheric blocks, and heated by radioactive decay. Following continental breakup at 105 Ma, slow outward drainage of this enriched and heated asthenosphere was channelled into thinner parts of the continental and

oceanic lithosphere. Sublithospheric drainage and decompression melting of this enriched mantle provides a viable explanation for these and many other intraplate magmatic occurrences.

1. Introduction

Plate tectonics accounts well for the volume and composition of magmas erupted at plate boundaries, but not for those erupted within plates. Small amounts of intraplate magma can be generated through lithospheric flexure or extension, but elevated mantle temperature (plumes or mantle "hotspots") is usually invoked to explain more voluminous intraplate magmatism. Intraplate ocean islands and seamounts are composed largely of basalt with a distinct composition that is shared by basalt forming continental intraplate volcanoes. Deep-seated, fixed mantle plumes ("hot spots") were originally proposed by Morgan (1971) as an explanation for long, time-progressive trails of volcanic ocean islands and seamounts. This model has evolved since then, and in its current form is often accepted as the standard explanation for virtually all oceanic intraplate volcanism (e.g. White, 2015). The assumption of a deep-mantle plume origin for ocean island basalt (OIB) has a profound impact on our understanding of the recycling of crust-derived material into the mantle. A plume origin for ocean islands with long, time-progressive aseismic ridges and island/seamount trails (e.g. Hawaii, Iceland, Réunion, Galapagos) is justifiable and well established, but these represent by no means all intraplate magmatism. Many intraplate occurrences still challenge the plume model, including the examples highlighted in this paper.

The Atlantic Ocean and its continental passive margins contain several intraplate volcanic centres, two of which straddle continental and oceanic lithospheres. Here we focus on the eruptive products of these two locations on the margins of the South Atlantic: the enigmatic

Cenozoic magmatic provinces of Northeast Brazil (NEB) and the Cameroon line (CL) (Figure 1). The regions were adjacent before continental separation in the Cretaceous and are the only significant occurrences of Cenozoic magmatic rocks on the two continental margins. We demonstrate that magmatic activity in these two areas was contemporaneous, started >45 Myr after continental separation, and is identical in incompatible-element concentrations. For the two provinces to have separate and unrelated causes would require an astonishing coincidence. An entirely new explanation is required that may be applicable to many other examples of intraplate magmatism and thus would require a re-evaluation of OIB and our understanding of crustal recycling into the deep mantle.

Here, we compare the geochemistry and chronology of the NEB and CL provinces using new and existing geochemical data, fifteen new $^{40}Ar/^{39}Ar$ ages obtained for NEB, including previously undated parts of the province, and published isotope data. Our new geochemical data were obtained using X-ray fluorescence (XRF) spectrometry in the same laboratory and using the same methods as previously published XRF data for the CL (Fitton and Dunlop, 1985; Fitton, 1987, 2007) allowing highly reliable comparisons between the two regions. Sample localities are shown in Figure 2. Locality coordinates and geochemical and geochronological data for a new suite of NEB rock samples are provided as supplementary material.

2. Methods

2.1 Element concentrations

All samples analyzed in this study were collected from NE Brazil. Forty-four samples from Fernando de Noronha and 29 from the continental sector of NE Brazil were prepared and analysed by X-Ray Fluorescence (XRF) at the University of Edinburgh. Major element concentrations were measured on fused glass discs and trace element concentrations on pressed powder pellets. Samples were analysed using a Philips PW2404 wavelengthdispersive sequential X-ray spectrometer fitted with a Rh anode end-window X-ray tube. Analytical methods are detailed in Fitton et al. (1998) and a full description of the XRF techniques and values of international geochemical reference standards analyzed with this study are provided in Supplementary file A together with sample localities and the analytical data.

2.2 $^{40}Ar/^{39}Ar$ dating

$^{40}Ar/^{39}Ar$ analyses and sample preparation were conducted at the Scottish Universities Environmental Research Centre (SUERC), East Kilbride. Dated samples include mafic and felsic groundmass, and sanidine crystals from phonolite samples. Fish Canyon sanidine (28.294 ± 0.036 (1σ) Ma; Renne et al., 2011, 2010; Schwarz et al., 2011) was used as a standard to monitor ^{39}Ar production and establish neutron flux values (J) for the samples. Gas was extracted from 50 mg sample aliquots via step-heating using a mid-infrared (10.6 μm) CO_2 laser with a non-Gaussian, uniform energy profile and a 3.5 mm beam diameter. Liberated Ar was purified of active gases and data were collected on a GVi Instruments ARGUS V multi-collector mass spectrometer using a variable sensitivity Faraday collector array in static collection (non-peak-hopping) mode (Sparks et al., 2008; Mark et al., 2009). All blank, interference and mass discrimination calculations were performed with the MassSpec software package (MassSpec, version 8.058, authored by Al Deino, Berkeley Geochronology Center, Version 8.058). Inverse-variance-weighted plateau ages were chosen as the best estimates of the emplacement ages. Table 1 contains a summary of the new age data. Heating profile results are presented in Supplementary file B.

3. The Cameroon line and NE Brazil magmatic provinces

The two provinces comprise suites of volcanic and plutonic igneous rocks that span the ocean-continent boundary, show no linear age progression and have experienced prolonged magmatic activity (Fitton, 1987; Knesel et al., 2011; Njome and de Wit, 2014; Perlingeiro et al., 2013; Silveira, 2006; Souza et al., 2013). The two areas were adjacent to one another before continental separation at ~105 Ma (Rabinowitz and LaBrecque, 1979). The CL is a prominent 1600-km-long volcanic lineament which stretches from the Atlantic island of Annobón to the interior of the African continent (Figure 1). CL magmatism started at about 65 Ma (Njome and de Wit, 2014), ~40 Myr after continental break-up, and continues to the present day with the active Mount Cameroon. NEB was magmatically active between ~52 and ~1 Ma and has surprisingly few plutonic rocks exposed at the surface (Silveira, 2006; Knesel et al., 2011; Perlingeiro et al., 2013; Souza et al., 2013). There are no other volumetrically comparable continental occurrences of Cenozoic volcanism along the entire Atlantic conjugate margins of South America and Africa. Both magmatic provinces are located over Proterozoic (Pan-African) fold belts situated adjacent to cratons (Figure 1).

The CL runs parallel to the Cretaceous Benue trough (Figure 1), which is the failed arm of a triple junction formed when Africa separated from South America. A marine incursion in the Turonian (~90 Ma) extended north-eastward from the Benue trough into a more extensive rift system that linked the South Atlantic and Tethys (Benkhelil, 1989). Subsidence and marine sediment deposition in the Benue trough ended at about 80 Ma with a phase of compression and folding (Benkhelil, 1989). The extensional phase of the Benue rift system thus predates the onset of CL magmatism by about 15 Myr. The CL volcanic rocks range in composition from transitional basalt to nephelinite and alkali rhyolite to phonolite, with an older suite of gabbro, syenite and alkali granite plutonic complexes (Fitton, 1987). Despite numerous attempts to explain the Cameroon line (reviewed by Njome and de Wit, 2014), its origin remains perplexing. The lack of age progression in the location of volcanism (the historically active Mount Cameroon is located in the centre of the line) and low $^3He/^4He$ (5.0–6.7 Ra; Barfod et al., 1999) are difficult to reconcile with a plume origin. The oceanic sector of the CL runs obliquely to ocean-floor transform faults (Figure 1), and there is no clear evidence for Cenozoic extensional faulting in the continental sector. Voluminous magmatism (four ocean islands and four large continental volcanoes) and longevity (~65 Myr) preclude an origin by lithospheric flexure as proposed for the so-called "petit-spot" seamounts in the NW Pacific Ocean (Hirano et al., 2006).

Cenozoic volcanism in NEB is comparatively limited geographically and volumetrically. It is mostly alkaline in composition and comprises three volcanic sub-provinces (Figure 2) adjacent to the Cretaceous Potiguar Basin (a continuation of the Benue trough in West Africa, Figure 1). These volcanic subprovinces are: (1) the Mecejana volcanic field, which includes a cluster of phonolite necks and plugs exposed over an area ~50 km around the city of Fortaleza; (2) the Macau-Queimadas volcanic lineament (MQVL), which is a chain of mostly basaltic necks, plugs and lava flows (alkali basalt to nephelinite) with rare trachyte dykes and gabbro intrusions extending from the town of Macau, Rio Grande do Norte, to Queimadas, Paraíba; and (3) Fernando de Noronha, an ~18 km^2 oceanic island that forms the easternmost edifice of a seamount chain continuing westwards towards Fortaleza with compositions ranging from alkali basalt to nephelinite and trachyte to phonolite. Fernando de Noronha is the only accessible offshore occurrence of Cenozoic volcanic rocks in the region. Magmatism in the south of the MQVL was associated with localised extensional tectonics around Boa Vista and Cubati (Souza et al., 2005, 2013). These are the only regions in both NEB and the CL where there is evidence for significant Cenozoic extension. Larger degree and shallower mantle melting beneath these areas has generated transitional basic and some sub-alkaline intermediate magmas with lower concentrations of incompatible elements than in mafic samples from the rest of the NEB and the CL (Figure 3).

4. Geochronology

Published $^{40}Ar/^{39}Ar$ ages for Fernando de Noronha indicate activity in two phases with a hiatus of ~3 Myr (Perlingeiro et al., 2013). The older period of volcanism occurred between 12.5 ± 0.1 Ma and 9.0 ± 0.1 Ma and the younger between 6.2 ± 0.1 Ma and 1.3 ± 0.1 Ma (Perlingeiro et al., 2013). $^{40}Ar/^{39}Ar$ dates for the MQVL range from 51.8 ± 0.9 Ma to 7.1 ± 0.3 (Silveira, 2006; Knesel et al., 2011; Souza et al., 2013), indicating synchronous Late Miocene volcanic activity in the MQVL and Fernando de Noronha, which are ~450 km apart. Fifteen new $^{40}Ar/^{39}Ar$ dates from groundmass and phenocryst phases for Mecejana and the MQVL are presented here (Table 1). Full analytical method and data reduction information are provided in Supplementary file C. New $^{40}Ar/^{39}Ar$ ages range from Late Eocene to Middle Miocene and are not geographically age progressive. In the Mecejana volcanic field, they range from 35.03 ± 0.28 Ma to 30.80 ± 0.22 Ma. In the central segment of the MQVL, they range from 33.99 ± 0.09 Ma to 12.39 ± 0.24 Ma, whereas in the northern and southern segments they are 21.60 ± 0.58 Ma (N) and 24.50 ± 0.08 Ma to 21.09 ± 0.05 Ma (S). New and previously published $^{40}Ar/^{39}Ar$ ages for the Cenozoic rocks of NE Brazil are shown in Figure 2, including those from the single intrusive province dated at 46 ±4 Ma (Silveira, 2006).

All available geochronological data for NEB and CL volcanic centres are summarised in Figure 4. The lack of age progression in the NEB and CL volcanic centres despite their longevity rules out involvement of deep mantle plumes in the two provinces. The CL includes plutonic complexes up to ~65 Ma (Fitton, 1987; Njome and de Wit, 2014) which are limited in NEB. The single dated plutonic occurrence from NEB has an age contemporaneous with similar complexes in the CL (Figure 4). The sparsity of such occurrences in NEB and the lack of ages for them may be the reason for the apparent later (~15 Myr) onset of activity there. The age distribution of the extrusive activity in the two provinces is remarkably similar (Figure 4), with magmatism starting in the continental sectors and then extending into the oceanic sectors 30–40 Myr later. The oldest available dates for either region postdate continental separation in the area (~105 Ma; Rabinowitz and LaBrecque, 1979) by at least 40 Myr, and reflect contemporaneous magmatic processes acting on two independent plates on precisely conjugate segments after a significant portion of the Atlantic Ocean basin (>2000 km) had formed (Figure 1).

5. Geochemistry

Mafic rocks (MgO ≥ 6 wt.%) from NEB and the CL (Fitton and Dunlop, 1985; Fitton, 1987, 2007) are virtually indistinguishable in their incompatible-element abundances, both between the two regions and between their respective oceanic and continental sectors (Figure 3), implying similar mantle-source compositions and melting processes for magmas in both provinces. Pb-isotope ratios are likewise indistinguishable between mafic rocks from Fernando de Noronha and those from the oceanic sector of the CL (Halliday et al., 1992), but significant differences are seen in Sr- and Nd-isotope ratios (Figure 5a). Sr- and Nd-isotope data from the continental sectors (not shown) are similar to data from their respective oceanic sectors but show more scatter due to contamination by continental crust (Gerlach et al., 1987; Halliday et al., 1988; Lee et al. 1994; Fodor et al., 1998).

Given the similarity in incompatible-element abundances (and hence parent/daughter ratios) between the two regions, the isotopic differences imply differences in the age of enrichment of the two mantle sources. Figure 5b shows estimates of the age of enrichment of depleted mantle (T_{DM}) as a function of the melt fraction represented by the NEB and CL magmas. The calculations were based on the average $^{143}Nd/^{144}Nd$ in mafic rocks from each of the two regions and a weighted average Sm/Nd for both data sets (Sm/Nd has similar values in the NEB and CL isotopic data set). For melt fractions of 0.01–0.02 (1–2%), T_{DM} for both CL and NEB coincides with the age range of the Panafrican orogenies, and the Nd-isotopic difference between the two provinces represents a difference in age of enrichment of ~200 Myr (Figure 5b). The Pb-isotope similarity between the two provinces and the overlap with mid-ocean ridge basalt (Halliday et al., 1992) implies that U,Th/Pb ratios were unaffected by this enrichment process.

6. Discussion and Conclusions

A genetic relationship between the two provinces has profound implications for the origin of intraplate magmatism in general. Since the two provinces were contiguous before continental break-up, they will have very similar lithospheric thicknesses in their respective oceanic and continental sectors. The indistinguishable incompatible-element composition of primitive magmas erupted in the two provinces (Figure 3) must therefore indicate the same range in partial melting (and therefore potential temperature, Tp) of compositionally similar mantle. Mantle Tp beneath the CL has been estimated, by applying PRIMELT3 (Herzberg and Asimow, 2015) to the composition of olivine-hosted melt inclusions, at 1350–1400°C (Ngwa et al., 2017), consistent with a non-plume origin. Attempts to apply the same procedure to whole-rock NEB analyses were unsuccessful due to clinopyroxene crystallization and/or because melting was influenced by volatiles. As was noted earlier, contemporaneous magmatism on precisely conjugate margins, the lack of age progression in either province, and the low $^{3}He/^{4}He$ in the CL, when taken together, effectively rule out the involvement of mantle plumes. But the volume and longevity of magmatism require some mechanism that can sustain a supply of geochemically and isotopically enriched mantle to the melt zones for at least 65 m.y. If this mantle isn't supplied from below via mantle plumes then is must be flowing in sideways under the lithosphere. Some form of lithospheric control on magmatism is required, but the strong compositional similarities between mafic volcanic rocks from the continental and oceanic sectors of the two margins requires that these have similar sublithospheric mantle sources. The ancient continental lithospheric mantle must be chemically and isotopically distinct from the younger, adjacent oceanic lithosphere and so, as was noted in the case of the Cameroon line by Fitton and Dunlop (1985) we can rule out *in situ* melting of the lithospheric mantle beneath the respective continental and oceanic sectors. The NEB and CL volcanic provinces are located along mobile belts between major cratonic blocks (Figure 1), suggesting that the causes, location and composition of magmatism may have been controlled by the architecture of the continental lithosphere.

The lithosphere-asthenosphere boundary zone (LABZ) coincides approximately with the region where the volatile-saturated mantle solidus intersects the geotherm (Figure 6), causing this zone to be enriched through small-degree melts rich in water, carbonate, and incompatible trace elements that percolate upwards until they reach their solidus temperature and freeze within the lower lithosphere (McKenzie, 1989). This carbonate-enriched zone will have a lower solidus temperature than normal mantle and provides a potential source for intraplate magmas. The assembly of Gondwana, completed by ~550 Ma, was accompanied by Pan-African (referred to as Brasiliano in South America) deformation and thickening of the lithosphere (Priestley et al., 2019). Enrichment through percolation (McKenzie, 1989) would be followed, over time, by thermal re-equilibration and conversion of this enriched lower lithospheric mantle into asthenosphere, once continental convergence and the thickening processes themselves have ceased. The newly created asthenosphere would be held in place by buoyancy (Priestley et al., 2019) and by the presence of adjacent lithospheric blocks, and would also be heated by radioactive decay. Mobilisation of this enriched asthenospheric mantle after Gondwana broke up, >400 Myr after final assembly, would allow it to drain slowly into adjacent areas of thinner lithosphere and partially melt (Figure 6). Oceanward flow of the relatively warm and volatile-enriched sub-Gondwana LABZ mantle would be channeled into the thinnest parts of the lithosphere, like an inverted drainage pattern (Ebinger and Sleep, 1998). This enables decompression melting beneath pre-existing thinner lithosphere leading to intraplate volcanism. Locations like the CL and NEB, which sit on the thinnest lithosphere on the South Atlantic margins (Priestley et al., 2019) between the thicker lithosphere of cratons (Figure 1), are favourable sites for such LABZ flow and consequent intraplate magmatism.

The isotopic composition of primitive NEB and CL magmas (Figure 5a) supports this explanation. Pan-African deformation and thickening of lithospheric mantle during the assembly of Gondwana would be followed by its enrichment via percolating carbonate-rich fluids (McKenzie, 1989), and this accounts for the late-Pan-African model ages (T_{DM}) of NEB and CL mafic rocks (Figure 5b). Isotopic differences and the ~200 Myr difference in T_{DM} between the two are consistent with the contrasting tectonic history of the Amazonia, West African and Congo-San Francisco cratonic blocks which surround the CL and NEB magmatic provinces (Figure 1). The assembly of Amazonia involved several orogenic episodes between ~2000 and 900 Ma before it joined Gondwana, whereas the West African and Congo-San Francisco cratons had stabilized long before the Pan-African orogenies (De Waele et al., 2008; Nance et al., 2019). The older T_{DM} and consequently the more enriched isotopic composition of the NEB mafic rocks (Figure 5) reflects the longer period of mantle enrichment around the Amazonia craton.

Our new model (Figure 6) accounts for the longevity of magmatism and the delay between the onset of magmatism in the continental and oceanic sectors in both the CL and NEB (Figure 4). It also resolves the long-standing problem of the relationship between the Benue trough and the CL (Fitton, 1980). Prolonged extension and subsidence in the Benue trough was virtually amagmatic except in the south-west part adjacent to the rift that developed into the South Atlantic (Benkhelil, 1989), and yet vigorous magmatism flared up 200 km to the south-east to form the parallel CL (Figure 1), 15 Myr after the end of basin subsidence, despite the apparent lack of local extensional faulting along the CL. The striking similarity in shape between the Benue trough and CL (Fitton, 1980; Figure 1) may be explained if Cretaceous extension in the former was due to simple shear along low-angle detachment faults resulting in an offset between the basin and thinning at the base of the lithosphere (Wernicke, 1981). If this is the case, then the CL magmatic flare-up coincides with the arrival of warm enriched asthenospheric mantle into the channel of thin lithosphere, firstly beneath Cameroon at ~65 Ma and subsequently beneath the new oceanic lithosphere (Figure 4). Continued oceanward flow may account for the diffuse field of seamounts extending from the end of the CL towards the Mid-Atlantic Ridge (Figure 1), and seamounts off the east coast of Brazil may have a similar origin.

Outflow of enriched asthenospheric mantle can also explain many other occurrences of intraplate magmatism around the dispersed fragments of Gondwana. The Cape Verde, Canary, and Madeira islands sit on lithosphere of similar age and may have formed when warm asthenosphere flowing away from the West African craton reached oceanic lithosphere thin enough for the asthenosphere to melt. Magmatism in the Atlas Mountains and east of Africa in Madagascar and the Comoro Islands may also be due to warm, enriched asthenosphere being channeled between cratonic blocks. Likewise, asthenospheric outflow from beneath North America may have been responsible for the New England seamounts and Bermuda. Some of these hotspots coincide with the location of broad vertical regions of reduced shear-wave velocity in the deep (>1000 km) mantle that have been identified as the roots of mantle plumes by French and Romanowicz (2015). These anomalous regions, however, are not seen to extend into the shallower mantle, many have no associated hotspot, and some well-established mantle plumes (e.g. Yellowstone) have no associated lower-mantle anomaly.

Our proposed solution to the conundrum of contemporaneous intraplate magmatism on precisely conjugate continental margins through a process of sublithospheric drainage could be widely applicable to occurrences where observations fail to support a deep mantle-plume origin or where such origin may be dubious. It provides a better alternative explanation for intraplate magmatism than edge-driven convection (e.g. Belay et al., 2019) because it can explain both the longevity and enriched composition of CL and NEB magmatism. Current ideas on the recycling of surface materials through the deep mantle are based on the assumption of plume involvement in most oceanic hotspot magmatism, and this assumption must be questioned.

Acknowledgements

Funds for the Ar dating were provided by the NERC Isotope Geosciences Steering Committee (IP-1568-1115). ARG and the geochemical analyses were supported through a University of Edinburgh Scholarship. We thank Nic Odling for his help with the XRF analyses, and Richard Ernst and Andy Saunders for their insightful reviews.

References

Barfod, D.N., Ballentine, C.J., Halliday, A.N., Fitton, J.G. (1999). Noble gases in the Cameroon line and the He, Ne, and Ar isotopic compositions of high μ (HIMU) mantle. J. Geophys. Res. 104, 29509–29527.

Belay, I.G., Tanaka, R., Kitagawa, H., Kobayashi, K., Nakamura, E., 2019. Origin of ocean island basalts in the West African passive margin without mantle plume involvement. Nature Commun. 10, 1–12. doi:10.1038/s41467-019-10832-7

Benkhelil, J., 1989. The origin and evolution of the Cretaceous Benue Trough (Nigeria). J. African Earth Sci. 8, 251–282. doi:10.1016/S0899-5362(89)80028-4

Bleeker, W., 2003. The late Archean record: A puzzle in ca. 35 pieces. Lithos 71, 99–134. doi:10.1016/j.lithos.2003.07.003.

Dasgupta, R. Hirschmann, M.M., 2010. The deep carbon cycle and melting in Earth's interior. Earth Planet. Sci. Lett. 298, 1–13.

De Waele, B., Johnson, S.P., Pisarevsky, S.A., 2008. Palaeoproterozoic to Neoproterozoic growth and evolution of the eastern Congo Craton: Its role in the Rodinia puzzle. Precamb. Res. 160, 127–194.

Ebinger, C.J., Sleep, N.H., 1998. Cenozoic magmatism throughout east Africa resulting from impact of a single plume. Nature 395, 788–791.

Fitton, J.G., 1980. The Benue trough and cameroon line - A migrating rift system in West Africa. Earth Planet. Sci. Lett. 51, 132–138. doi:10.1016/0012-821X(80)90261-7

Fitton, J.G., 1987. The Cameroon line, West Africa: a comparison between oceanic and continental alkaline volcanism, in: Fitton, J.G., Upton, B.G.J. (Eds.), Alkaline Igneous Rocks. Geological Society, London, pp. 273–291. doi:10.1144/GSL.SP.1987.030.01.13

Fitton, J.G., 2007. The OIB paradox, in: Foulger, G.R., Jurdy, D.M. (Eds.), Plates, Plumes and Planetary Processes. The Geological Society of America, pp. 387–412. doi:10.1130/2007.2430(20)

Fitton, J.G., Dunlop, H.M., 1985. The Cameroon line, West Africa, and its bearing on the origin of oceanic and continental alkali basalt. Earth Planet. Sci. Lett. 72, 23–38.

doi:10.1016/0012-821X(85)90114-1

Fitton, J.G., Saunders, A.D., Larsen, L.M., Hardarson, B.S., Norry, M.J., 1998. Volcanic rocks from the southeast Greenland Margin at 63°N: composition, petrogenesis, and mantle sources. Proc. Ocean Drill. Program, Sci. Results 152. doi:10.2973/odp.proc.sr.152.233.1998.

Fodor, R.V., Mukasa, S.B., Sial, A.N., 1998. Isotopic and trace-element indications of lithospheric and asthenospheric components in Tertiary alkalic basalts, northeast Brazil. Lithos 43, 197–217.

French, S.W., Romanowicz, B., 2015. Broad plumes rooted at the base of the Earth's mantle beneath major hotspots. Nature 525, 95–99.

Gerlach, D.C., Stormer, J.C., Mueller, P. a., 1987. Isotopic geochemistry of Fernando de Noronha. Earth Planet. Sci. Lett. 85, 129–144. doi:10.1016/0012-821X(87)90027-6

Griffin, W.L., O'Reilly, S.Y., Afonso, J.C., Begg, G.C., 2009. The composition and evolution of lithospheric mantle: a re-evaluation and its tectonic implications. J. Petrolgy 50, 1185–1204.

Halliday, A.N., Davies, G.R., Lee, D.-C., Tommasini, S., Paslick, C.R., Fittont, J.G., Jamest, D.E., 1992. Lead isotope evidence for young trace element enrichment in the oceanic upper mantle. Nature 359, 623–627.

Halliday, A.N., Dickin, A.P., Fallick, A.E., Fitton, J.G., 1988. Mantle dynamics: A Nd, Sr, Pb and O isotopic study of the Cameroon line volcanic chain. J. Petrol. 29, 181–211. doi:10.1093/petrology/29.1.181

Herzberg, C., Asimow, P.D., 2015. PRIMELT3 MEGA.XLSM software for primary magma calculation: Peridotite primary magma MgO contents from the liquidus to the solidus. Geochemistry, Geophys. Geosystems 563–578. doi:10.1002/2014GC005631

Hirano, N., Takahashi, E., Yamamoto, J., Abe, W., Ingle, S.P., Kaneoka, I., Hirata, T., Kimura, J.I., Ishii, T., Ogawa, Y., Machida, S., Suyehiro, K., 2006. Volcanism in response to plate flexure. Science (80-.). 313, 1426–1428. doi:10.1126/science.1128235

Klein, E.L., Moura, C.A.V., 2008. São Luís Craton and Gurupi belt (Brazil): Possible links with the West African Craton and surrounding Pan-African belts. Geol. Soc. Spec. Publ. 294, 137–151. doi:10.1144/SP294.8

Knesel, K.M., Souza, Z.S., Vasconcelos, P.M., Cohen, B.E., Silveira, F. V., 2011. Young volcanism in the Borborema Province, NE Brazil, shows no evidence for a trace of the Fernando de Noronha plume on the continent. Earth Planet. Sci. Lett. 302, 38–50. doi:10.1016/j.epsl.2010.11.036

Kröner, A., Stern, R.J., 2004. Pan-African orogeny. Encyclopedia of Geology 1, Amsterdam, Elsevier, 1–12, in: Selley, R.C., Cocks, R., Plimer, I. (Eds.), Encyclopedia of Geology. Elsevier, Amsterdam, pp. 1–12.

Lee, D.C., Halliday, A.N., Fitton, J.G., Poli, G., 1994. Isotopic variations with distance and time in the volcanic islands of the Cameroon line: evidence for a mantle plume origin. Earth Planet. Sci. Lett. 123, 119–138. doi:10.1016/0012-821X(94)90262-3

Mark, D.F., Barfod, D., Stuart, F.M., Imlach, J., 2009. The ARGUS multicollector noble gas mass spectrometer: Performance for 40Ar/39Ar geochronology. Geochemistry, Geophys. Geosystems 10. doi:10.1029/2009GC002643

McDonough, W.F., Sun, S. s., 1995. The composition of the Earth. Chem. Geol. 120, 223–253. doi:10.1016/0009-2541(94)00140-4

McKenzie, D., 1989. Some remarks on the movement of small melt fractions in the mantle. Earth Planet. Sci. Lett. 95, 53–72. doi:10.1016/0012-821X(89)90167-2

McKenzie, D., O’Nions, R.K., 1991. Partial melt distribution from inversion of rare earth element concentrations. J. Petrol. 32, 1021–1091. doi:10.1093/petrology/32.5.1021

Morgan, W.J., 1971. Convection plumes in the lower mantle. Nature 230, 42–43. doi:10.1038/229560a0

Müller, R.D., Sdrolias, M., Gaina, C., Roest, W.R., 2008. Age, spreading rates, and spreading asymmetry of the world's ocean crust. Geochemistry, Geophys. Geosystems 9, 1–19. doi:10.1029/2007GC001743

Nance, R.D., Murphy, J.B., Strachan, R.O.B.A., Keppie, J.D., Gutie, G., Rez, J.F.N., Quesada, C., Linnemann, U.L.F., Lemos, R.D., Pisarevsky, S.A., Sciences, E., Francis, S., Scotia, N., 2019. Neoproterozoic – early Palaeozoic tectonostratigraphy and palaeogeography of the peri-Gondwanan terranes : Amazonian v . West African connections ´ a , Universidad Nacional Autonoma de Me 345–383.

Ngwa, C.N., Hansteen, T.H., Devey, C.W., van der Zwan, F.M., Suh, C.E., 2017. Origin and evolution of primitive melts from the Debunscha Maar, Cameroon: Consequences for mantle source heterogeneity within the Cameroon Volcanic Line. Lithos 288–289, 326–337. doi:10.1016/j.lithos.2017.06.028

Njome, M.S., de Wit, M.J., 2014. The Cameroon Line: Analysis of an intraplate magmatic province transecting both oceanic and continental lithospheres: Constraints, controversies and models. Earth-Science Rev. 139, 168–194. doi:10.1016/j.earscirev.2014.09.003

Perlingeiro, G., Vasconcelos, P.M., Knesel, K.M., Thiede, D.S., Cordani, U.G., 2013. 40Ar/39Ar geochronology of the Fernando de Noronha Archipelago and implications for the origin of alkaline volcanism in the NE Brazil. J. Volcanol. Geotherm. Res. 249, 140–154. doi:10.1016/j.jvolgeores.2012.08.017

Pin, C., Bassin, C., 1992. Evaluation of a strontium-specific extraction chromatographic method for isotopic analysis in geological materials. Anal. Chim. Acta 269, 249–255. doi:10.1016/0003-2670(92)85409-Y

Pin, C., Zalduegui, J.F.S., 1997. Sequential separation of light rare-earth elements, thorium and uranium by miniaturized extraction chromatography: Application to isotopic analyses of silicate rocks. Anal. Chim. Acta 339, 79–89. doi:10.1016/S0003-2670(96)00499-0

Priestley, K., Mckenzie, D., Ho, T., 2019. A Lithosphere – Asthenosphere Boundary — a Global Model Derived from Multimode Surface - Wave Tomography and Petrology, in: Yuan, H., Romanowicz, B. (Eds.), Lithospheric Discontinuities, Geophysical Monograph 239, American Geophysical Union. John Wiley & Sons.

Rabinowitz, P.D., LaBrecque, J., 1979. The Mesozoic South Atlantic Ocean and Evolution of Its Continental Margins. J. Geophys. Res. 84, 5973–6002.

Renne, P.R., Balco, G., Ludwig, K.R., Mundil, R., Min, K., 2011. Response to the comment by W.H. Schwarz et al. on "Joint determination of 40K decay constants and 40Ar*/40K for the Fish Canyon sanidine standard, and improved accuracy for 40Ar/39Ar geochronology" by P.R. Renne et al. (2010). Geochim. Cosmochim. Acta 75, 5097–5100. doi:10.1016/j.gca.2011.06.021

Renne, P.R., Mundil, R., Balco, G., Min, K., Ludwig, K.R., 2010. Joint determination of 40K decay constants and 40Ar*/40K for the Fish Canyon sanidine standard, and improved accuracy for 40Ar/39Ar geochronology. Geochim. Cosmochim. Acta 74, 5349–5367. doi:10.1016/j.gca.2010.06.017

Schwarz, W.H., Kossert, K., Trieloff, M., Hopp, J., 2011. Comment on the " Joint determination of 40K decay constants and 40Ar*/40K for the Fish Canyon sanidine standard, and improved accuracy for 40Ar/39Ar geochronology" by Paul R. Renne et al.

(2010). Geochim. Cosmochim. Acta 75, 5094–5096. doi:10.1016/j.gca.2011.06.022

Silveira, F. V, 2006. Magmatismo cenozóico da porção central do Rio Grande do Norte, NE do Brasil. `universidade Federal do Rio Grande do Norte.

Souza, Z.S. de, Nascimento, M.A.L. do, Barbosa, R.V.N., Dias, L.G. da S., 2005. Geology and tectonics of the Boa Vista Basin (Paraíba, northeastern Brazil) and geochemistry of associated Cenozoic tholeiitic magmatism. J. South Am. Earth Sci. 18, 391–405. doi:10.1016/j.jsames.2004.11.007

Souza, Z.S. de, Vasconcelos, P.M., Knesel, K.M., Dias, L.G. da S., Roesner, E.H., Farias, P.R.C. de, Morais Neto, J.M. de, 2013. The tectonic evolution of Cenozoic extensional basins, northeast Brazil: Geochronological constraints from continental basalt 40Ar/39Ar ages. J. South Am. Earth Sci. 48, 159–172. doi:10.1016/j.jsames.2013.09.008

Sparks, R.S.J., Folkes, C.B., Humphreys, M.C.S., Barfod, D.N., Clavero, J., Sunagua, M.C., McNutt, S.R., Pritchard, M.E., 2008. Uturuncu volcano, Bolivia: Volcanic unrest due to mid-crustal magma intrusion. Am. J. Sci. 308, 727–769. doi:10.2475/06.2008.01

Walter, M.J., 1998. Melting of garnet peridotite and the origin of komatiite and depleted lithosphere. J. Petrol. 39, 29–60. doi:10.1093/petroj/39.1.29

Wernicke, B., 1981. Low-angle normal faults in the Basin and Range Province: nappe tectonics in an extending orogen. Nature 291, 645–648.

White, W.M., 2015. Isotope Geochemistry. John Wiley & Sons, Oxford.

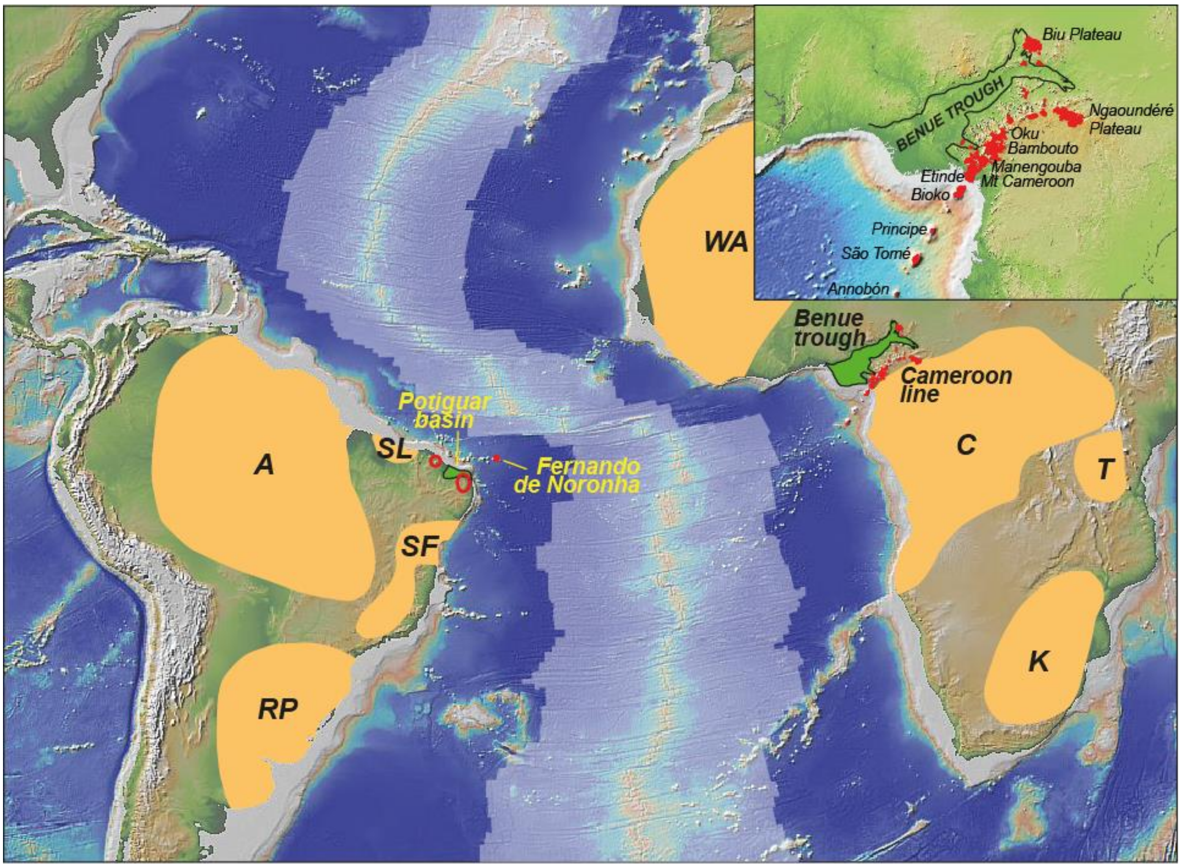

Fig. 1. Map of the South Atlantic Ocean showing the location of the Cameroon line and the NE Brazil volcanic provinces. A more detailed map of the Cameroon Line is given as an inset. Volcanic rocks of the Cameroon line are marked in red; those in NE Brazil are too small to show individually so the main areas are circled in red. Orange areas are Archaean cratonic blocks (Bleeker, 2003; Klein and Moura, 2008): A, Amazonia; SL, São Luís; SF, São Francisco; RP, Rio de la Plata; WA, West Africa; C, Congo, T, Tanzania; K, Kalahari. The shaded area in the centre of the ocean is bounded by magnetic anomaly 31 (67.7 Ma; Müller et al., 2008) and shows the amount of seafloor created since the onset of magmatism on the Cameroon line.

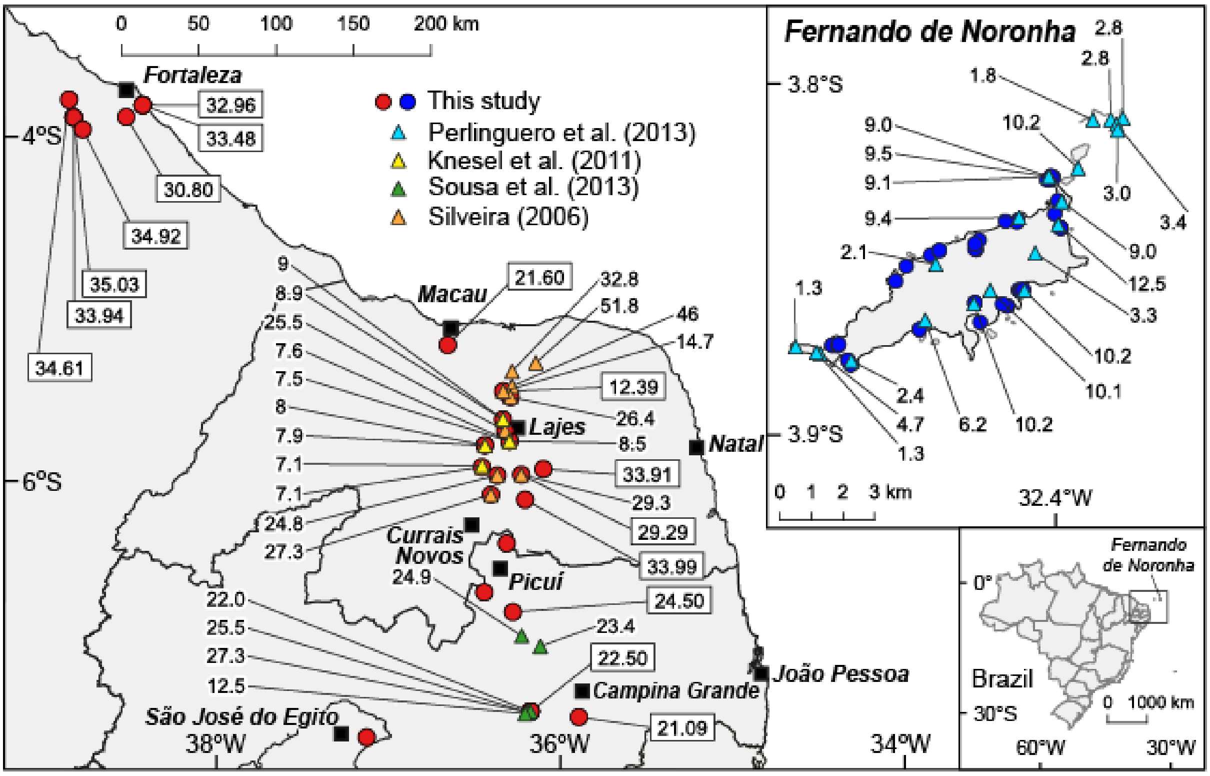

Fig. 2. Map of Northeast Brazil showing all the available $^{40}Ar/^{39}Ar$ ages (in Ma) for the Cenozoic lava flows and intrusive rocks in the region, based on the results of this (ages in boxes) and other studies (Knesel et al., 2011; Perlingeiro et al., 2013; Silveira, 2006; Souza et al., 2013). All the samples collected during this study (red and blue circles) were analyzed for major- and trace-elements. M, Mecejana; MQVL, Macau-Queimadas volcanic lineament. The two insets show the position of the region on a map of Brazil, and Fernando de Noronha on a larger scale. Full details of the Ar analyses are given as supplementary material.

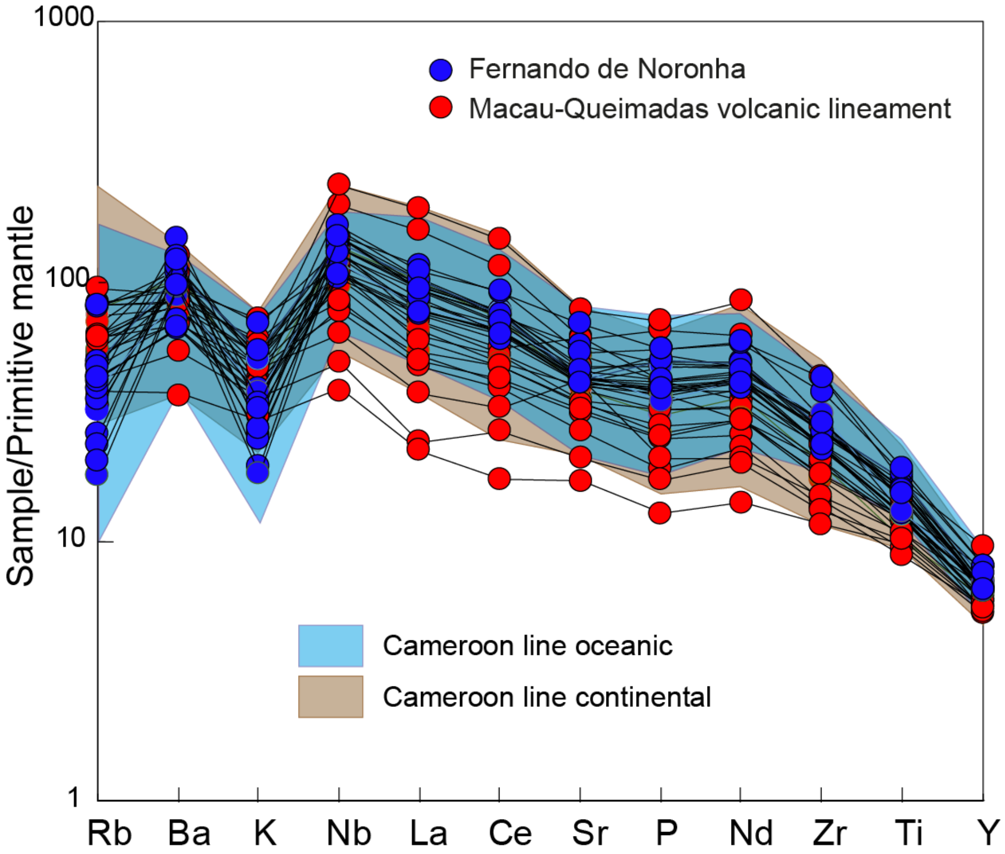

Fig. 3. Primitive-mantle-normalized incompatible trace-element abundances (PM values from McDonough and Sun, 1995) in basalt samples with MgO>6 wt.% from NE Brazil and the Cameroon line. The fields for the Cameroon line continental and oceanic basalt is based on data in Fitton (2007). Note the striking similarity in basalt composition from the Cameroon line and NE Brazil and between the continental and oceanic sectors in both provinces. The

two NEB samples with relatively low incompatible-element abundances are transitional basalt associated with local extension in the southern part of the MQVL.

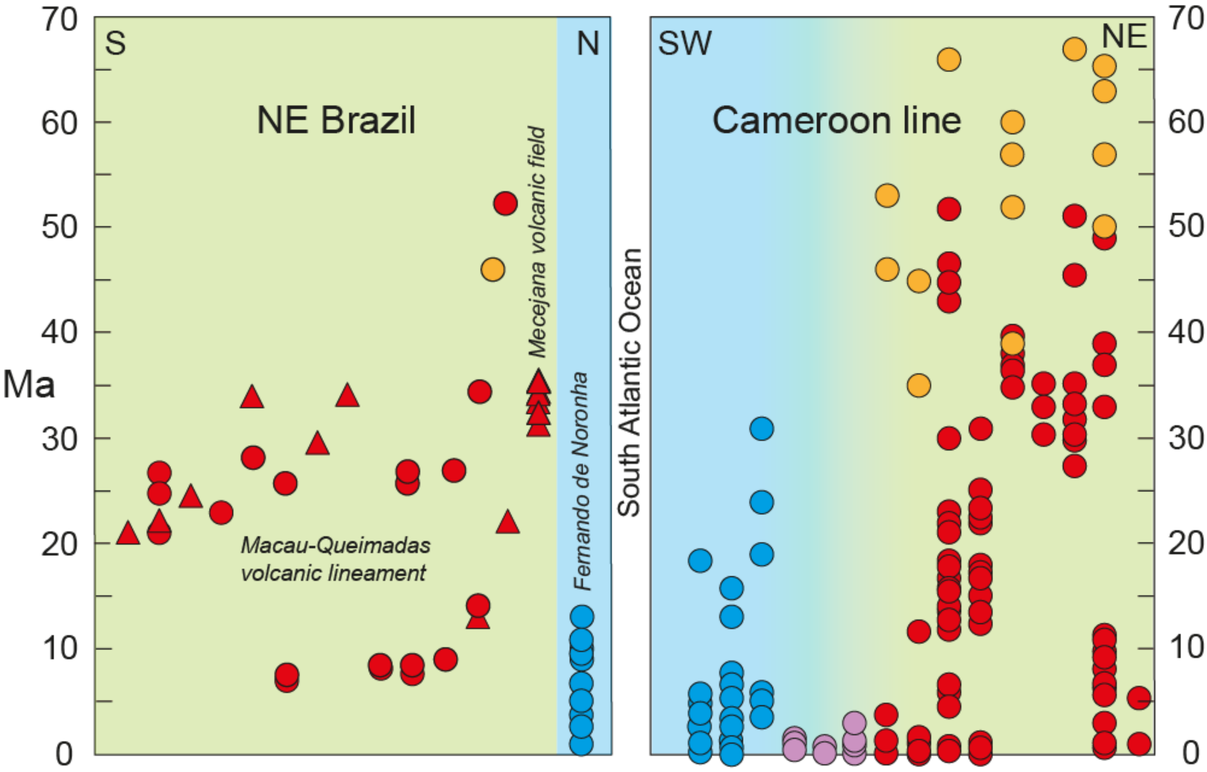

Fig. 4. A summary of age data for Cenozoic volcanic rocks from the Cameroon line (Njome and de Wit, 2014) and NE Brazil (Knesel et al., 2011; Perlingeiro et al., 2013; Silveira, 2006; Souza et al., 2013). Continental volcanic rocks are indicated by red symbols (red triangles are new dates reported here), orange symbols indicate plutonic rocks, blue symbols are oceanic volcanic rocks, and purple symbols represent lava samples from Mount Cameroon, Etinde and Bioko on the Cameroon line continent–ocean transition.

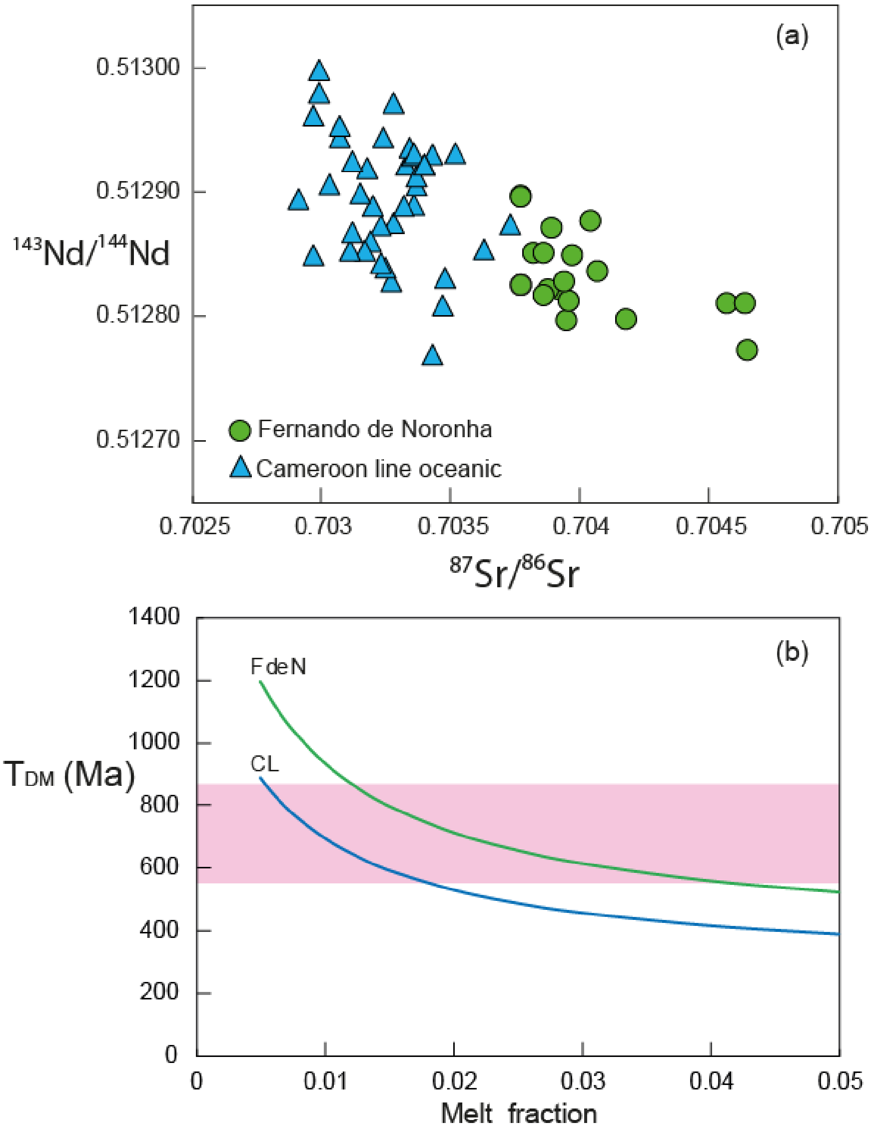

Fig. 5. (a) Sr- and Nd-isotopic data for Fernando de Noronha (oceanic NEB; Gerlach et al., 1987) and the oceanic sector of the CL (Halliday et al., 1988; Lee et al., 1994. (b) Model mantle enrichment age (T_{DM}) as a function of the melt fraction represented by the NEB and CL magmas. T_{DM} is the time at which the Nd-isotope growth curve for a NEB or CL mantle source with average values of $^{143}Nd/^{144}Nd$ (0.51283 and 0.51290, respectively) intersects the growth curve for depleted mantle (present-day $^{147}Sm/^{144}Nd$=0.2238 and $^{143}Nd/^{144}Nd$=0.5131). Source Sm/Nd was calculated as a function of melt fraction from the weighted mean NEB and CL Sm/Nd (0.196) assuming non-modal batch melting of garnet peridotite:

$$(Sm/Nd)_{source} = (Sm/Nd)_{liquid}\,(D_{Sm}+F-P_{Sm}F)/(D_{Nd}+F-P_{Nd}F)$$

where D is the mean distribution coefficient weighted by the proportion of mineral phases, P is the mean distribution coefficient weighted by the proportion that each phase contributes to the melt, and F is the melt fraction. Phase proportions and D values were taken from McKenzie and O'Nions (1991) and melting proportions from Walter (1998). Increasing melt fraction increases mantle Sm/Nd and decreases T_{DM}. The isotopic difference between primitive oceanic NEB and CL rocks requires a difference in enrichment age of ~200 Myr. The pink band represents the age range (870–550 Ma) of the Pan-African orogenic events (Kröner and Stern, 2004).

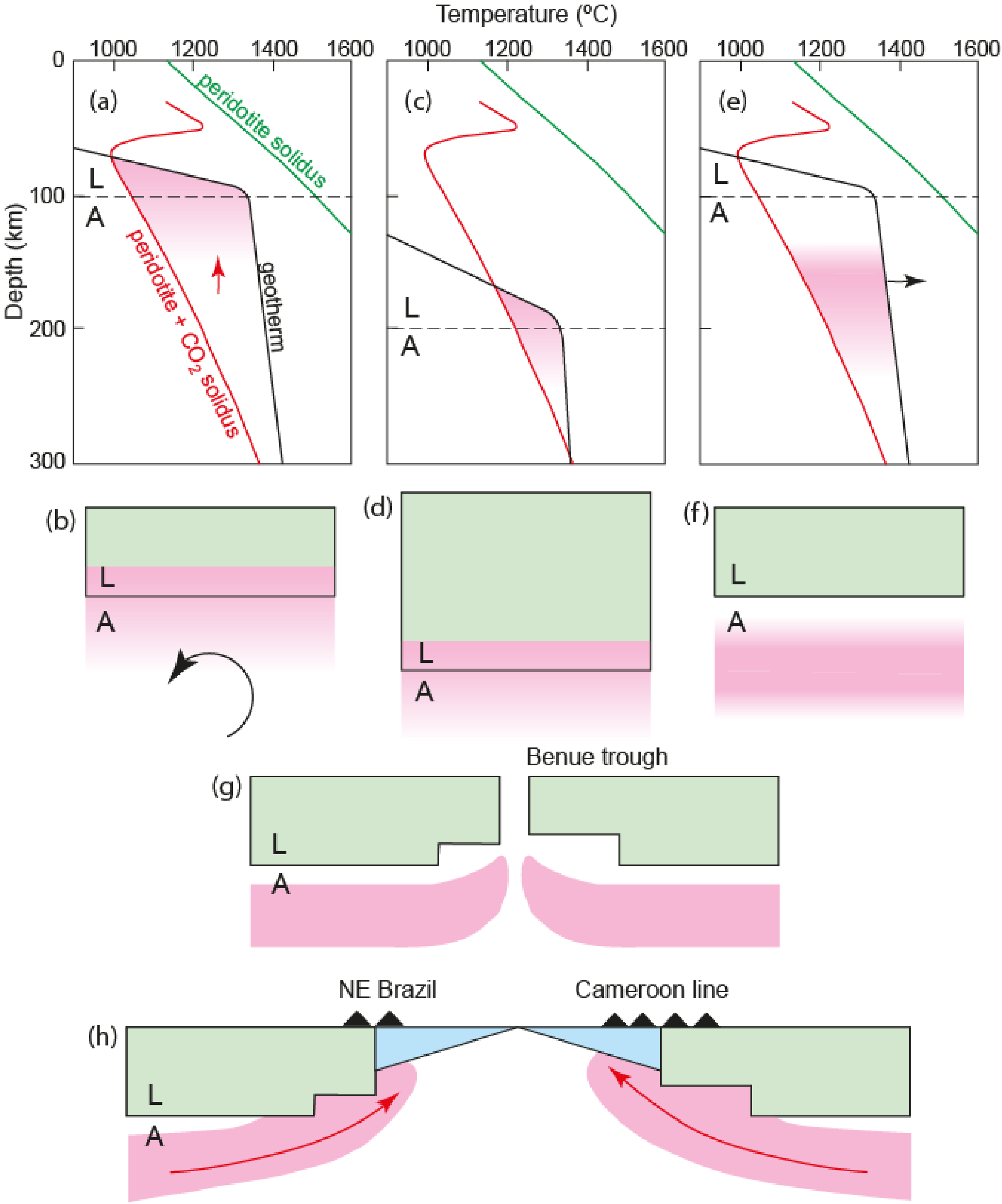

Fig. 6. Conceptual framework for the origin of Cameroon line and NE Brazil magmatism. (a) Depth-temperature diagram and (b) schematic section through the lithosphere (L) and asthenosphere (A) for the initial conditions with lithosphere 100 km thick and a mantle potential temperature of 1300°C. The peridotite solidus and its solidus in the presence of CO_2 are from Dasgupta and Hirschmann (2010). Small-degree carbonate melt, formed by reaction

between CO_2 and clinopyroxene, will be present in lherzolite mantle where the geotherm oversteps the peridotite + CO_2 solidus and will percolate upwards (red arrow) to enrich the lower lithospheric mantle and underlying asthenosphere (pink). Convective overturn restricts build-up of carbonate melt in the asthenosphere. (c,d) The effects of lithospheric thickening to 200 km accompanying the assembly of Gondwana from 870–550 Ma. (e,f) Over time the thickened lithosphere warms by conduction and, in the enriched parts, by radioactive decay, and its lower part converts to asthenosphere. The formation and percolation of new carbonate melt in the converted lithosphere is inhibited by its composition which becomes increasingly depleted (harzburgitic) upwards (Griffin et al., 2009). The carbonate-enriched layer is therefore isolated within the new asthenosphere (f) and is held in place by buoyancy and prevented from dispersing by adjacent lithospheric blocks. (g) Continental breakup at 105 Ma is accompanied by the formation of the Benue trough and its continuation in NE Brazil, creating regions of thinner lithosphere that will provide the locus of future magmatism. (h) Subsequent seafloor spreading creates new oceanic lithosphere (blue). The carbonate-enriched asthenosphere must be sufficiently viscous for it to remain attached to the overlying plates as they drift apart. It drains slowly out from beneath the continental lithosphere and melts beneath regions of thinner continental and oceanic lithosphere, leading to the formation of the Cameroon line and NE Brazil magmatic provinces from ~65 and ~52 Ma, respectively. The isolation and viscosity of the enriched layer of asthenosphere (f) accounts for the ~40 m.y. delay between the start of seafloor spreading and the onset of CL and NEB magmatism.

Table 1: Summary of $^{40}Ar/^{39}Ar$ age results for samples from Northeast Brazil. Full results and further sample information, including coordinates, are given as supplementary material. Sample localities are shown in Figure 2. gm = groundmass; snd = sanidine phenocryst. *Plateau calculation uses trapped composition determined from isochron analysis rather than the isotopic composition of air.

Sample	Rock type	Material	Plateau age (Ma) ±2σ	Integrated age (Ma) ± 2σ	Isochron age (Ma) ± 2σ
MQVL					
15BP3-2	alkali basalt	gm	**21.09 ± 0.05**	21.1 ± 0.2	20.87 ± 0.22
15BP3-3b	basaltic andesite	gm	**22.50 ± 0.32***	25.0 ± 3.8	22.50 ± 2.65
15BP3-5	basalt	gm	**24.50 ± 0.08**	24.4 ± 0.5	24.55 ± 0.11
15BP5-8	basanite	gm	**33.99 ± 0.09**	32.9 ± 1.9	33.97 ± 0.08
15BP5-9	basanite	gm	**33.91 ± 0.94**	35.2 ± 4.1	33.51 ± 1.67
15BP5-10	basanite	gm	**29.29 ± 0.11**	28.9 ± 0.5	29.15 ± 0.19
15BP7-14	basaltic andesite	gm	**21.60 ± 0.58**	21.0 ± 0.8	21.45 ± 0.24
15BP7-15	nephelinite	gm	**12.39 ± 0.24**	12.36 ± 0.84	12.50 ± 0.29
Mecejana					
15BP9-19a	phonolite	snd	**33.48 ± 0.15**	33.4 ± 0.3	33.57 ± 0.14
15BP9-19c	phonolite	gm	**32.96 ± 0.15**	32.9 ± 0.4	32.97 ± 0.16
15BP10-20(b)	phonolite	snd	**30.80 ± 0.22**	34.0 ± 0.5	31.22 ± 0.33
15BP10-21a	phonolite	snd	**33.94 ± 0.25**	34.0 ± 0.5	33.98 ± 0.27
15BP10-21b	phonolite	snd	**35.03 ± 0.28**	35.0 ± 0.2	35.03 ± 0.24
15BP10-22(b)	phonolite	snd	**34.92 ± 0.27***	35.7 ± 1.3	34.92 ±0.41
15BP10-23	phonolite	snd	**34.61 ± 0.23**	34.6 ± 0.2	34.62 ± 0.17